Image enhanced polymer-based multimode interference coupler covering *C* and *L* bands using deeply etched air trenches

Xiaolong Wang and Ray T. Chen[a)]
Microelectronic Research Center, the University of Texas at Austin, 10100 Burnet Rd., MER 160, Austin, Texas 78758

(Received 14 November 2006; accepted 11 February 2007; published online 13 March 2007)

A design of multimode interference coupler with deeply etched air trenches at the boundary of the multimode section is proposed for photonic integrated circuitry on low-index-contrast materials. The device length decreases from 820 to 750 μm for a 1×8 polymer multimode interference coupler. Due to the enhanced optical confinement, the optimized coupler with air trenches experimentally achieved 0.28/0.23 dB reduced insertion loss, 2.16/2.34 dB improved contrast ratio for transverse-electric and transverse-magnetic polarization, compared with conventional multimode interference coupler. The device entirely covers the wavelength range of both *C* and *L* bands, which is sufficient for broadband communications. © *2007 American Institute of Physics*.
[DOI: 10.1063/1.2713626]

Multimode interference (MMI) couplers are widely used in many photonic integrated circuits (PICs), such as power splitters,[1] optical switches,[2] and phased array multiplexers.[3] Based on the self-imaging principle,[4] MMI couplers offer the advantages of compact size, low cross-talk, and low power imbalance. Compared to directional couplers and *Y* splitters, MMI couplers show superiority in scalability, since they do not need to be cascaded in order to achieve large port counts. Theoretical work in Ref. 5 suggested means to improve image quality in terms of two physical sources, namely, larger mode counters and smaller phase errors. Higher-order guided waves offer a better image resolution due to their higher spatial frequency, while smaller phase error among different guided modes is paramount for large port counts. Both of these two performance-limiting factors require a high index contrast in the multimode section. MMI devices fabricated on III-V semiconductor compounds[6] and silicon-on-insulator[7] yield good image quality. Although these devices can achieve ultracompact size, their submicron cross section induces higher propagation loss and low coupling efficiency with single mode fibers. Low-index-contrast materials, for example, silica[8] and polymer[9] devices, have gained distinguished popularity in the past decades due to their low insertion loss and polarization insensitivity. The square cross-section channel waveguide provides a good profile matching with the fundamental mode of an optical fiber. To improve image quality, polymer MMI devices using metal cladding to obtain a strong lateral confinement were proposed in Ref. 10. However, metal cladding limits device operation to a single polarization due to metallic absorption of transverse-magnetic (TM) waves. A more attractive approach with the introduction of deeply etched air trenches at the boundary of multimode section was proposed in Refs. 11 and 12 independently. Their simulations predict improved image quality without sacrifices in coupling efficiency. But until now, no experimental results have confirmed this optimized design. In this letter, we apply the proposed design to a 1×8 MMI coupler as a specific case. Using a three-dimensional semivector beam propagation method (3D SVBPM), we compare the performance in terms of loss, power imbalance, and contrast ratio, for the devices with and without air trenches. The optimized MMI couplers fabricated on ultraviolet (UV) curable fluorinated polymers demonstrate improved image quality compared with conventional MMI couplers on the same chip, which agrees with the simulation results.

A 1×8 MMI coupler is illustrated in Fig. 1. Conventional MMI couplers, as Fig. 1(a) shows, have a core refractive index of n_0 and cladding index of n_1, both for the input waveguide and the multimode section. Detailed analysis of the self-imaging property is presented in Ref. 4. A basic expression for the field profile $\psi(x,y,z)$ at a distance $z=L$ is written as

$$\psi(x,y,z)=\sum_{\nu=0}^{m-1} c_\nu \psi_\nu(x,y)\exp[j(\beta_0-\beta_\nu)z], \tag{1}$$

where ν is the guided mode sequence number, m is the total excited mode number, ψ_ν is the νth excited mode profile, c_ν is the excitation coefficient, β_ν is the propagation constant, and

$$\beta_\nu \approx k_0 n_0 - \frac{(\nu+1)^2\pi\lambda}{4n_0 W_\nu^2}, \tag{2}$$

where $k_0=\lambda/2\pi$, W_ν is the effective width for mode m including the penetration depth due to the Goose-Hahnchen shift. To ensure good image quality, there must first be a sufficient number of guided modes, i.e., m must be large enough to increase the spatial resolution of the reproduced image; and second, sufficiently small phase error, which means $\beta_0-\beta_\nu$ has harmonic beat length for different ν, so that

$$\beta_0-\beta_\nu \approx \frac{\nu(\nu+2)^2\pi}{3L_\pi}, \tag{3}$$

where $L_\pi=\pi/(\beta_0-\beta_1)=4n_0W_0^2/3\lambda_0$ is the beat length of the two lowest-order modes. This approximation requires the penetration depth of each guided mode below submicron scale. Both of these two criteria require a strong index contrast in the multimode section.

[a)]Electronic mail: chen@ece.utexas.edu

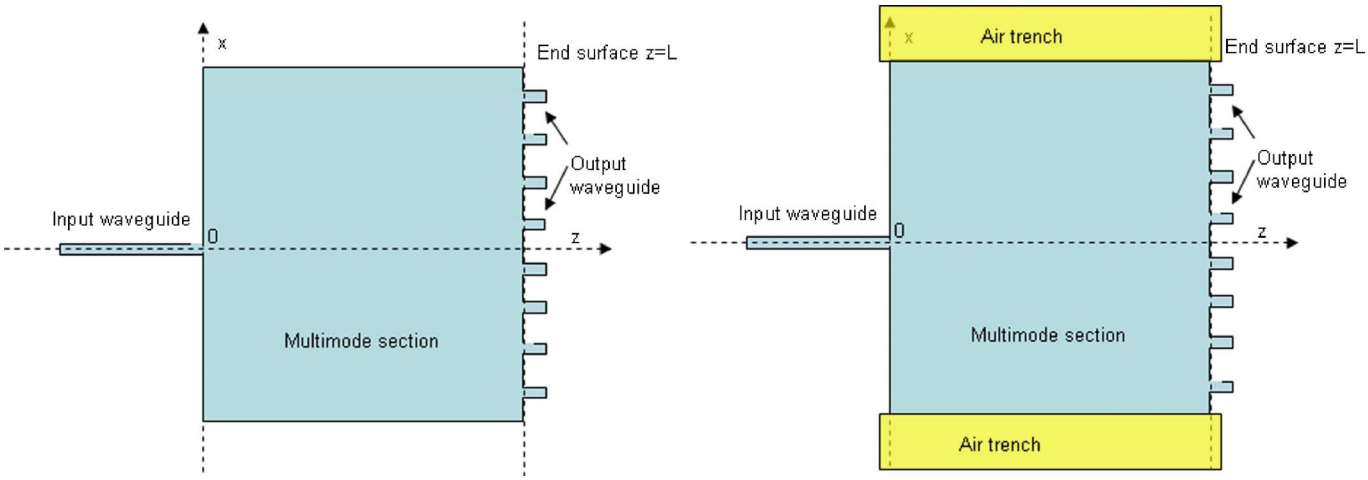

FIG. 1. (Color online) Schematics of (a) conventional MMI coupler and (b) optimized MMI coupler with air trenches.

When air trenches are introduced to define the edges of the MMI coupler, which is shown in Fig. 1(b), more guided modes can be excited, and lateral penetration depth into the cladding is substantially reduced so that the effective width of all the guided modes is approximately the same as the actual width of the MMI coupler. Hence, the presence of air trenches improves image quality.

3D SVBPM is employed to simulate the performance of the MMI couplers. The refractive indices of the cladding and core are 1.45 and 1.46, respectively. The center-positioned input waveguide has 5×5 μm^2 cross section, and the width of the multimode section is 80 μm. The lengths of the multimode sections of the two designs are 820 and 750 μm, respectively. Air trenches are placed adjacent to the multimode section and deeply etched to the substrate. The near field images of the TM mode at the end surface of the multimode sections are displayed in Fig. 2. For conventional MMI couplers, the weakest intensity contrast ratio (CR) is 5.74 dB, where CR is defined as CR $=10\log(peakintensity/adjacentvallyintensity)$. The power imbalance is 0.48 dB and excess loss is 0.23 dB. As a comparison, the optimized MMI coupler achieves a CR of 8.53 dB, power imbalance of 0.45 dB, and excess loss of 0.07 dB. The power imbalance is not significantly improved as Refs. 11 and 12 show, since 3D BPM is adopted instead of two-dimensional BPM used in those references. The performance of the transverse-electric (TE) mode, together with the experimental results, is summarized in Table I.

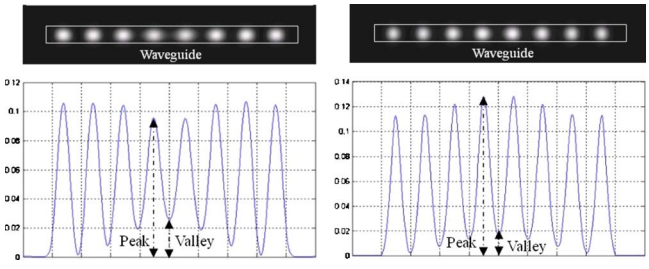

FIG. 2. (Color online) Near field image intensity of (a) conventional MMI coupler and (b) optimized MMI coupler with air trenches.

ZPU12-RI series polymer materials from ChemOptics are employed to make the optical waveguide on a silicon wafer. First, a layer of ZPU12-450 ($n=1.45$ at 1550 nm wavelength) as the bottom cladding is spin coated onto the wafer. After UV curing and thermal baking, a second layer of ZPU12-460 ($n=1.46$) is spun which serves as the core layer. A suitable thickness of SiO_2 as a hard masking material is then deposited and patterned by a dry etching method. Once the hard mask is properly defined, reactive ion etching (RIE) is used to form the channel waveguides in the core material. The remaining hard mask is then removed by wet etching and a polymer top cladding layer is spin coated and cured. To introduce the air trenches, another layer of SiO_2 hard mask is grown and patterned to open the trench windows. The polymer is then completely etched down to the silicon bottom in the RIE chamber. The fabricated sample is cleaved and both ends are polished. In order to monitor the near field image of the MMI coupler, the output plane is exactly polished to the

TABLE I. Simulation and experimental result of the 1×8 MMI coupler.

	Conventional MMI coupler				Optimized MMI coupler			
	TE		TM		TE		TM	
	Sim.	Expt.	Sim.	Expt.	Sim.	Expt.	Sim.	Expt.
Excess loss (dB)	0.15	2.03	0.23	1.57	0.01	1.75	0.07	1.34
Power imbalance (dB)	0.51	0.98	0.48	0.78	0.73	0.84	0.45	0.75
Contrast ratio (dB)	5.71	3.08	5.74	2.63	9.74	5.24	8.53	4.97

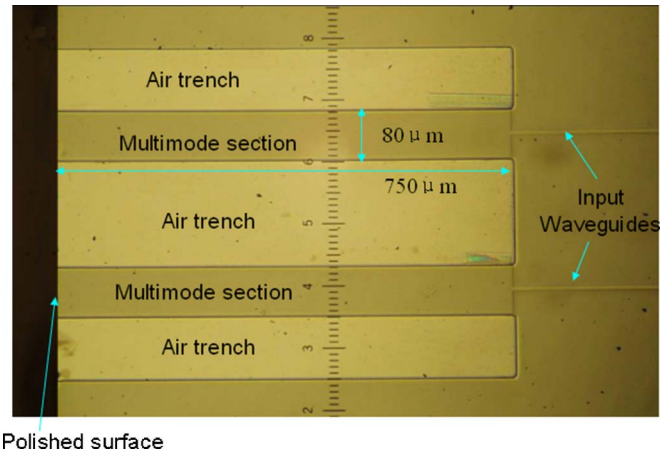

FIG. 3. (Color online) Microscopy of the fabricated 1×8 MMI couplers with air trenches.

end surface of the multimode waveguide, as shown in Fig. 3.

The chip is vacuum mounted on the holder of a Newport PM500C autoaligner, and a 9 μm core diameter single mode fiber is precisely positioned to couple the 1550 nm wavelength laser to the input waveguide. A 40× lens is closely placed to the polished surface to project the near field image onto a charge coupled device camera. The TM mode intensity profile of a conventional MMI coupler without any air trenches and the optimized MMI coupler are shown in Figs. 4(a) and 4(b), respectively. This polarization independent device shows a similar image profile for the TE mode, as detailed in Table I.

The wavelength response of the optimized MMI coupler is depicted in Fig. 5. The "channel output" represents the optical power from the centermost channel in Fig. 4(b), which is normalized to the maximum throughput power. Within the *C* and *L* bands, the channel output variation is less than 1 dB. The rapid power drop beyond 1490 and 1610 nm is a result of material absorption loss.[13] The "channel uniformity" in Fig. 5 is defined as the power ratio between the centermost and edgemost channels, irrespective of material absorption. The channel uniformity varies from

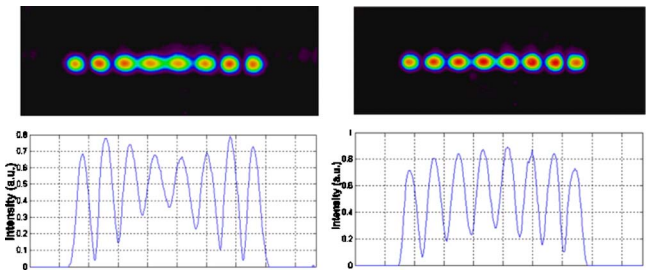

FIG. 4. (Color online) Near field images of (a) conventional MMI coupler and (b) optimized MMI coupler with air trenches.

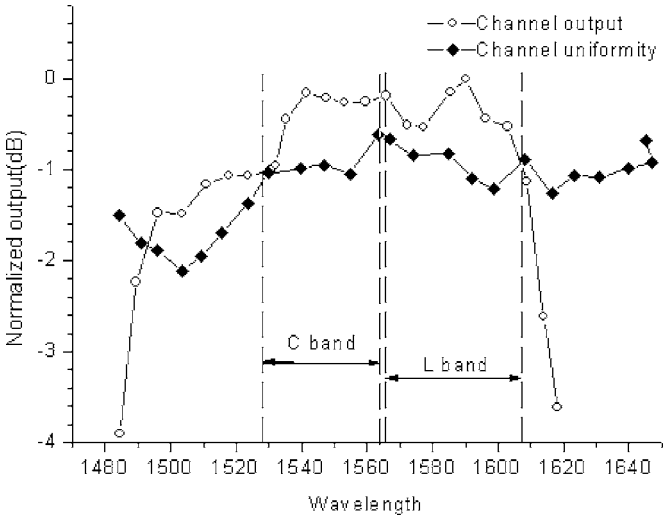

FIG. 5. Wavelength response of the optimized MMI coupler.

−1 to −0.6 dB in the *C* and *L* bands and can extend to a much longer wavelength range, proving the device architecture to be wavelength insensitive.

To conclude, we realized the theoretically optimized design of a 1×8 polymer MMI coupler by the introduction of deeply etched air trenches. Experimental results show that insertion loss reduced by 0.46 dB in the optimized MMI coupler and contrast ratio for the TE mode improved by 1.16 dB compared to conventional MMI couplers. For the TM polarization, the insertion loss reduced 0.31 dB and the contrast ratio improved by 2.34 dB. The device shows stable performance across the *C* and *L* band communications windows. The enhanced image quality will provide a higher potential for MMI couplers in large scale PICs.

[1] B. Li, S. J. Chua, E. A. Fitzgerald, B. S. Chaudhari, S. Jiang, and Z. Cai, Appl. Phys. Lett. **85**, 1119 (2004).
[2] J. Yu, X. Wang, J. Liu, Q. Yan, J. Xia, Z. Fan, Z. Wang, and S. Chen, Proceedings of the Sixth Chinese Symposium, Optoelectronics, p. 251.
[3] L. O. Lierstuen and A. Sudbo, IEEE Photonics Technol. Lett. **7**, 1034 (1995).
[4] L. B. Soldano and C. M. Pennings, J. Lightwave Technol. **13**, 615 (1995).
[5] J. Z. Huang, R. Scarmozzino, and R. M. Osgood, IEEE Photonics Technol. Lett. **10**, 1292 (1998).
[6] E. C. M. Pennings, R. J. Deri, A. Scherer, R. Bhat, T. R. Hayes, N. C. Andreadakis, M. K. Smit, L. B. Soldano, and R. J. Hawkins, Appl. Phys. Lett. **59**, 1926 (1991).
[7] H. Wei, J. Yu, X. Zhang, and Z. Liu, Opt. Lett. **26**, 878 (2001).
[8] H. N. J. Fernando, M. Hayden, and P. J. Hughes, Proc. SPIE **6183** (2006).
[9] A. V. Mule, R. Villalaz, T. K. Gaylord, and J. D. Meindl, IEEE Photonics Technol. Lett. **16**, 2490 (2004).
[10] J. Z. Huang, M. H. Hu, J. Fujita, R. Scarmozzino, and R. M. Osgood, IEEE Photonics Technol. Lett. **10**, 561 (1998).
[11] X. Wang and J. Yu, Acta Photonica Sin. **32**, 1045 (2003).
[12] C. J. Kaalund and Z. Jin, Opt. Commun. **250**, 292 (2005).
[13] X. Wang, B. Howley, M. Chen, and R. T. Chen, J. Lightwave Technol. **24**, 1558 (2006).